AIChE

Hindered Diffusion of Residue Narrow Cuts Through Polycarbonate Membranes

Zhentao Chen, Chunming Xu, Jinsen Gao, Suoqi Zhao, and Zhiming Xu
State Key Laboratory of Heavy Oil Processing, China University of Petroleum, Beijing 102249, P.R. China

DOI 10.1002/aic.12124
Published online January 8, 2010 in Wiley InterScience (www.interscience.wiley.com).

Hindered diffusion plays an important role in catalytic processing of residue and heavy oil because of large size molecules in these feedstocks. Vacuum residue of Athabasca oil sand bitumen was fractionated into 13 narrow fractions and an end-cut by supercritical fluid extraction and fractionation (SFEF). Diffusion transport of five SFEF cuts through four polycarbonate membranes was investigated using a diaphragm cell at 308 K. The results showed that diffusion coefficients of the five SFEF cuts decreased as the experiment proceeded, which illustrates that these cuts are polydisperse in size. The effective diffusion coefficients varied with molecular size and pore size. Hindered diffusion of the five SFEF cuts is significant in the membranes with nominal pore diameter of 15 nm, which is around the average pore size of typical hydrotreating catalyst. Comparisons between experimental data and theoretical prediction revealed that the actual hindered degree for diffusion of the five SFEF cuts is higher than that calculated by the Renkin equation. There were slight differences in diffusivity among saturate, aromatic, and resin constituents. © 2010 American Institute of Chemical Engineers *AIChE J,* 56: 2030–2038, 2010

Keywords: hindered diffusion, diffusion coefficient, membrane, residue, configuration effect

Introduction

As stocks of high-quality crude oil are exhausted, heavier petroleum feedstocks are being used to produce liquid fuels. As a result, effective conversion of these feedstocks to clean fuels has become one of the most critical issues in the petroleum processing industry. It is well known that the size of most residue species is comparable to the average pore diameters of typical upgrading catalysts. This causes hindered diffusion to occur during the catalytic conversion process. Resistance to diffusion would significantly reduce the effectiveness of the catalysts and the overall reaction rate. Therefore, the diffusion behavior of heavy petroleum is crucial to the design of efficient catalysts and the effective utilization of the feedstocks.

Correspondence concerning this article should be addressed to C. Xu at xcm@cup.edu.cn.

Although several advanced instruments have been used to measure diffusivities of asphaltenes in bulk solutions,[1,2] the hindered or restrictive diffusion coefficients of heavy oil molecules through porous materials cannot be determined from these methods. There have been three primary methods used to study the hindered diffusion behavior of asphaltenes and residue, which are described later.

In the first method, the effective diffusion coefficients of heavy oils through membranes are determined by a diaphragm diffusion cell. Baltus and Anderson[3] measured the diffusivity of five asphaltene fractions using track-etched mica membranes. A significant pore size effect on diffusional transport of the solute has been found from their results. Sane et al.[4–6] investigated the diffusion of asphaltenes through track-etched polycarbonate membranes. The results showed that the effective diffusion coefficient of asphaltenes varies as a function of experimental time. Knowledge of the structure of asphaltenes and the distribution of heteroatoms within asphaltenes has also been gained from their diffusion experiments.

Hindered diffusion of asphaltenes has also been studied by the adsorptive uptake method. Yang and Guin[7,8] investigated the effective diffusivities of coal and petroleum asphaltenes through a commercial catalyst. The results of their study indicated that the diffusion coefficients span one order of magnitude for coal asphaltenes fractions and more than two orders of magnitude for petroleum asphaltenes fractions. Mieville et al.[9] determined the diffusivities of petroleum asphaltenes through catalysts by uptake experiments. They found that Hondo asphaltenes have the highest diffusivities, which was attributed to their smaller particle sizes.

Thirdly, studies on asphaltenes and heavy petroleum diffusivities have been performed by using reactive kinetic data. Tsai et al.[10] investigated the restrictive diffusion of residual oils by a trickle bed reactor. The results showed that the restrictive diffusion effect is significant for hydrodesulfurization (HDS) and hydrodemetalation reactions. Yang et al.[11] studied the kinetics of HDS and hydrodenitrogenation (HDN) for narrow fractions of various residues. They found that HDS and HDN reactivities decreased as the molecular weight of residue fraction increased. The decreased reactivities were due to increased diffusion resistance and decreased intrinsic reactivity.

In the past, most studies have been performed on hindered diffusion of asphaltenes. In view of the importance of efficient utilization of residues, the diffusional transport of the entire residue should be obtained. However, because of the presence of a large number of different compounds in an actual feed material, it is extremely difficult to obtain meaningful data for the residue diffusion without an appropriate separation technique. With supercritical fluid extraction and fractionation (SFEF), it is possible to separate a residue into multiple narrow fractions with increasing molecular weight and polarity.[12] These narrow fractions can be used to investigate the diffusion behavior of the entire residue.

The hindered effect has been observed for the diffusion of heavy petroleum molecules in porous materials. The hindrance factor, the ratio of effective to bulk diffusion coefficient, has been commonly used to quantitatively describe the hindered degree of diffusion. Most hindered diffusion studies attributed hindrance to two factors: steric restriction or steric partition coefficient and hydrodynamic drag resistance. It is important to note that both of these factors depend on the ratio of solute size to pore size, $\lambda = d/d_p$. Here, d and d_p are molecule size and pore size, respectively.

Numerous theoretical correlations have been proposed to relate hindrance factor to λ. Combining equilibrium partition coefficient from Ferry and centerline drag coefficients from Lane allowed Renkin to obtain the relationship[13]

$$D_e/D_b = F(\lambda) = (1-\lambda)^2(1 - 2.104\lambda + 2.09\lambda^3 - 0.95\lambda^5), \quad (1)$$

where D_e is the effective diffusion coefficient of solute, D_b is the bulk diffusion coefficient of solute, and $F(\lambda)$ is the hindrance factor of diffusion. The Renkin equation is considered accurate for $\lambda < 0.5$. Good agreement between the Renkin equation and experimental data has been observed.[14,15] However, there are also some results, which were not in good agreement with the Renkin equation.[10,16] Several alternative empirical expressions have been developed. The following power-law relationship is one which has been used in hindered diffusion studies.[10,17]

$$F(\lambda) = (1-\lambda)^m. \quad (2)$$

The parameter m indicates the hindered magnitude of diffusion. A value of $m = 4.4$ approaches the predicted result of the Renkin equation.

In this study, the effective diffusion coefficients of five SFEF cuts for Athabasca oil sand bitumen vacuum residue (AVR) were measured by a diaphragm diffusion cell using polycarbonate membranes with nominal pore sizes of 15, 50, 80, and 1000 nm. The hindrance factors of the five SFEF cuts diffusing through the four porous membranes were determined.

Experimental

Feedstock preparation

Athabasca oil sand bitumen vacuum residue was obtained from the Syncrude oilsands plant in Fort McMurray, Alberta, Canada. The residue was separated into 13 narrow fractions and an end-cut by SFEF. The separation process and operating procedure have been reported elsewhere.[12,18]

It is known that the properties, such as molecular weight, of SFEF fractions vary gradually with increased SFEF yield. Hence, four narrow fractions (SFEF-3, SFEF-6, SFEF-9, and SFEF-12) and the end-cut of AVR were chosen as feedstocks for the diffusion experiments. The AVR and the corresponding five SFEF cuts (four fractions and the end-cut) were subjected to various analyses. The average molecular weight was determined in toluene at 45°C by using a Knauer vapor pressure osmometer. Saturates, aromatics, resins, and asphaltenes (SARA) analyses were performed according to the procedures described by Liang.[19]

Toluene was used as the solvent for the diffusion experiments. The end-cut solution was filtered through a 2-μm pore size filter before preparation. A 10 g/l solution of each feedstock in toluene was agitated at room temperature for 24 h.

Diaphragm diffusion cell

The apparatus is shown in Figure 1. The diaphragm diffusion cell contains two glass chambers, which are clamped together with a membrane between them. Teflon-coated magnetic stirring bars are mounted in the chambers and driven by the rotation of an external magnet. To eliminate boundary layer resistance, a fixed blade was placed about 2 mm away from the membrane surface. The speed of rotation of the stirring bar could be varied from 50 to 500 rpm (revolutions per minute) and controlled at any fixed value. To keep temperature constant, the cell was placed in a thermostatic bath during each experiment.

The lower and upper chamber hold a volume of 48.1 and 55.3 ml, respectively, which were measured by weighing the cell before and after filling with deionized water. Track-etched nuclepore polycarbonate membranes with nominal pore diameters of 15, 50, 80, and 1000 nm (Whatman) were used in the diffusion experiments. These types of membranes

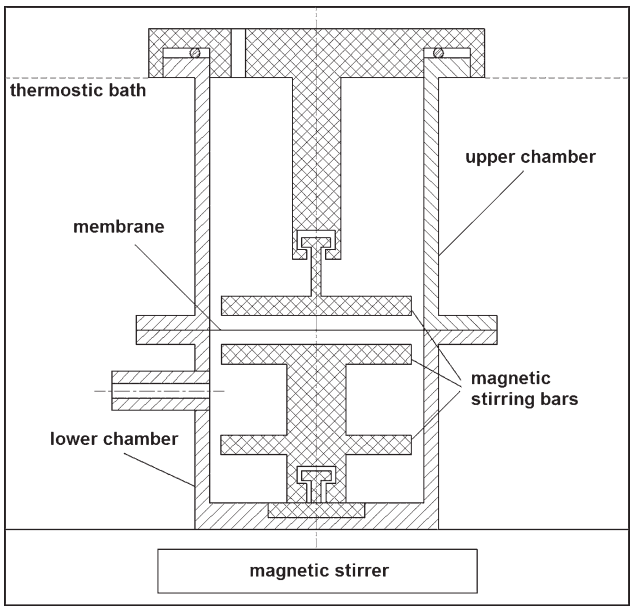

Figure 1. Diaphragm diffusion cell apparatus.

are extensively used in diffusional transport because of their ideal pore geometry.[16,20,21]

Calibration of the diaphragm cell constant

For calibration of the diaphragm cell constant, the lower chamber was filled with higher concentration solution of KCl (c_{L0} = 0.6 mol/l) and the upper chamber was filled with lower concentration solution of KCl (c_{U0} = 0.4 mol/l). The upper chamber was rinsed three times after preliminary diffusion and recharged with 0.4 mol/l KCl solution. After 0.5 h, the experiment was ended and samples from each chamber were taken for concentration analysis.

Diffusion coefficient measurements

The diffusion coefficient measurements were performed using the diaphragm of diffusion cell (Figure 1). The procedure used for the diffusion experiments was similar in each case. Initially, the lower chamber was filled with solution and the upper chamber was filled with pure solvent. Such a design can reduce convective transport.[22]

For the five SFEF cuts, discrete samples (about 2 ml) were withdrawn from the upper chamber at appropriate time intervals. Then, an equal volume of pure toluene was added to the upper chamber to keep the volume constant. The diffusion experiment ended when equilibrium was approached. The concentrations of the samples and the final solutions in the upper and lower chambers were determined by evaporating the solvent and weighing the solids. The concentration in the lower chamber was calculated from the mass balance.

In the pseudosteady state, the flux across the membrane in a time dt equals the change in the amount of solute in two chambers, so

$$-V_L \frac{dc_L}{dt} = D\frac{S}{l}(c_L - c_U) \tag{3}$$

$$V_U \frac{dc_U}{dt} = D\frac{S}{l}(c_L - c_U), \tag{4}$$

where c_L and c_U refer to solute concentrations in the lower and the upper chambers of the diaphragm cell, V_L and V_U are volumes of the lower and upper chamber, S is the effective diffusion area of the membrane pores, and l is the effective diffusion path length. There are two main assumptions in the above two equations. First, diffusion should approach steady state when one measures the diffusion coefficient. This can be achieved after preliminary diffusion in our experiments according to Gordon's correlation.[23] Second, the diffusion coefficient of the solute does not vary much with concentration of the residue cuts. In a recent study, Durand et al.[2] reported that the diffusion coefficients of petroleum fractions varied slightly in the 0–10 wt % range. Also, our results indicated that the diffusion coefficients of the SFEF cuts are similar at concentrations ranging from 10 to 50 g/l.

Combining Eqs. 3 and 4, one has

$$\frac{d}{dt}(c_L - c_U) = -\beta D(c_L - c_U), \tag{5}$$

where β is the constant of the diaphragm cell and is given by Eq. 6:

$$\beta = \frac{S}{l}\left(\frac{1}{V_L} + \frac{1}{V_U}\right). \tag{6}$$

Integrating Eq. 5 between the jth and $(j + 1)$th sampling, we have:

$$\ln\frac{c_{L,j+1} - c_{U,j+1}}{c_{L,j} - c_{U,j}} = -\beta D_j \Delta t_{j,j+1} (j = 0, 1, 2\ldots\ldots). \tag{7}$$

In this equation, the subscripts j and $j + 1$ refer to the sampling numbers, t is the time of sampling, and D_j is the average diffusion coefficient of the solute transporting through the pores between the jth and $(j + 1)$th sampling.

The mass balances were checked for the diffusion experiments. The results show that the mass of the solute in the lower chamber at the beginning of the experiment equal the mass of the solute in both chambers at the end of the experiment and in the samples. The differences of the mass measurements are less than 0.6%.

Hydrodynamic diameter measurements

The Brownian motion of a solute in a dilute solution due solely to the thermal fluctuations of the molecular movements around the solute can be described by the well-known Stokes-Einstein equation:

$$D_b = \frac{\kappa T}{3\pi\eta d}, \tag{8}$$

where κ is Boltzmann's constant, T is the absolute temperature, η is the solvent viscosity, and d is the diameter for a spherical solute or the equivalent hydrodynamic diameter for a nonspherical solute. According to Eq. 8, the hydrodynamic

Table 1. Properties of AVR and the Five SFEF Cuts

Properties	AVR	SFEF-3	SFEF-6	SFEF-9	SFEF-12	End-Cut
Molecular weight	1147	643	748	903	1599	8061
Saturates/% (mass)	7.80	14.78	5.07	0	0	0
Aromatics/% (mass)	41.52	68.03	63.32	61.43	48.15	5.80
Resins/% (mass)	32.60	18.16	31.41	38.13	58.72	18.84
Asphaltenes/% (mass)	18.09	0	0	0	0	75.86

diameter of the molecules can be determined by using the bulk diffusion coefficient of solute at infinite dilution.

Results and Discussion

Properties of the residue and the five SFEF cuts

The properties of the residue and the five SFEF cuts are summarized in Table 1. There are large variation in the properties of the four SFEF fractions and the end-cut. Molecular weight increases as the fractions become heavier. The average molecular weight of the end-cut is much larger than that of the four SFEF fractions. Asphaltene, which is the heaviest component in the residue, is concentrated in the end-cut.

Diaphragm cell constant

The presence of boundary layer resistance is observable in a diaphragm cell.[24] This effect can be reduced by stirring the blade close to membrane surface.[25,26] Several stirring speeds were evaluated for this study. The total diffusivity was constant at a stirring rate ranging from 90 to 120 rpm (revolutions per minute). Therefore, a stirring rate of 105 rpm was selected for this study.

As can be seen from Eq. 6, β is determined by the properties of the used membrane and the diaphragm cell. The value of β can be obtained by measuring these properties directly[27] or using a substance whose diffusion coefficients are known.[28] An aqueous solution of potassium chloride at 25°C was used to determine β in this study. The method is described elsewhere,[29–31] and the results corresponding to different pore sizes are provided in Table 2.

The diffusion coefficient of potassium chloride determined in our experiment is in agreement with the literature values,[28,32] 1.84–1.85 $\times$ 10^{-5} cm^2/s, using a similar concentration range. The cell constants were reproducible for all four membranes.

As mentioned earlier, the β values can be determined from Eq. 6 by measuring the properties of membranes directly. Three large pore size membranes (50, 80, and 1000 nm) were characterized as to pore length, average pore size, and pore density by scanning electron microscopy (SEM) photographs. Pore length was determined by measuring the membrane length from cross sections. Average pore diameter was determined from three SEM photographs containing more than 30 pores. Pore density was determined by counting the number of pores in the SEM photographs. The values of β determined from these properties are listed in Table 3.

The set of values of β in Table 3 is close to the calibrated values in Table 2. However, sharp SEM photographs could not be obtained for the 15-nm pore size membrane. As a result, the average values of the diaphragm cell constants from the calculations in Table 2 were used for all four membranes.

Effective diffusion coefficients

The effective diffusion coefficients of the four SFEF fractions and the end-cut at 308 K through the four membranes are plotted against the time in Figures 2–5.

The diffusion coefficients of each cut through each membrane are time dependent. The diffusion coefficients decrease gradually as the experiment proceeds. This illustrates that these cuts are polydisperse mixtures, which contain a large number of substances with different diameters. The smaller species diffuse more readily through the membrane pores, resulting in the decrease of the diffusion coefficients as the experiment progresses. Comparison of these figures shows that the effective diffusion coefficients for the same cut decrease with decreasing membrane pore diameters. The diffusion coefficients of the five SFEF cuts through the same membrane decrease as they become heavier. The decreasing trend of diffusion coefficients between two chosen adjacent cuts is greater as the cuts become heavier.

Sakai et al.[33] found that there was a downward curvature in the plot of the $\ln\Delta c(t)/\Delta c(t_i)$ vs. $(t - t_i)$ for fractioned petroleum pitch. The variation is slight because of the narrow fraction used in their study. Sane et al.[4] discovered the variations in diffusivity vs. time for Hondo California asphaltene.

Table 2. Calibration Data of the Diaphragm Cell Constant for Different Membranes

Membrane	C_{L0} (mol/l)	C_{U0} (mol/l)	C_{Lf} (mol/l)	C_{Uf} (mol/l)	$D \times 10^5$ (cm^2/s)	β (cm^{-2})	$\overline{\beta}$ (cm^{-2})
15-1	0.591	0.400	0.538	0.446	1.85	5.54	5.53
15-2	0.583	0.400	0.518	0.457	1.85	5.52	
50-1	0.577	0.400	0.521	0.448	1.85	26.67	26.64
50-2	0.577	0.400	0.520	0.447	1.85	26.61	
80-1	0.574	0.400	0.515	0.449	1.85	29.07	28.90
80-2	0.574	0.400	0.516	0.449	1.85	28.72	
1000-1	0.582	0.400	0.522	0.449	1.85	27.26	27.25
1000-2	0.581	0.400	0.523	0.449	1.85	27.24	

Table 3. Diaphragm Cell Constants Determined by Properties of Membranes

d_n* (nm)	d_m** (nm)	$n \times 10^{-8}$ (cm^{-2})	l (nm)	S (cm^2)	V_L (cm^3)	V_U (cm^3)	β (cm^{-2})
50	46.9	15.33	6.64	0.378	48.1	55.3	22.22
80	71.9	7.21	6.66	0.368	48.1	55.3	21.57
1000	852.0	0.14	11.01	0.972	48.1	55.3	34.46

*Norminal pore diameters of reported by the manufacturer.
**Pore diameters determined from SEM photographs.

The diffusion coefficients of asphaltenes through a 400-nm pore size membrane ranged from 2×10^{-6} to 8×10^{-6} cm^2/s, which varied more than that of the SFEF cuts used in this experiment. This may be because the asphaltenes used in their study are broader in size than the five SFEF cuts used in our experiments.

Asphaltenes and residue are known to readily associate in organic solvent. Recent studies have suggested that asphaltenes might aggregate at concentrations of 10–100 mg/l.[34–36] However, the diffusion coefficients of the SFEF cuts in this study do not vary even at concentrations up to 20 g/l. This implies that the molecules of the SFEF cuts might not aggregate under the conditions of our experiments. The existence of aromatic and resin components in the cuts and shear force created by agitators might contribute to eliminating aggregation of residue molecules.

Average effective diffusion coefficients

Although there is a diffusivity distribution for each cut across any membrane, the variation of the diffusion coefficient of any cut in each membrane is slight. Therefore, to quantitatively compare the diffusion transport ability between the different cuts, the average effective diffusion coefficient of each cut was defined by Eq. 9.

$$\overline{D_{e,i}} = \frac{\sum_{j=1}^{n} (D_{i,j} \times m_{i,j})}{\sum_{j=1}^{n} m_{i,j}} \quad (i = 3, 6 \ldots \text{end-cut}; j = 1, 2 \ldots n), \tag{9}$$

where $\overline{D_{e,i}}$ is the average effective diffusion coefficient of the ith cut and $m_{i,j}$ is the amount of the ith cut through the membrane in the jth interval. The calculated average effective diffusion coefficients of the five SFEF cuts are listed in Table 4.

The values of average effective diffusivity decrease not only as the five SFEF cuts become heavier but also as the membrane pore diameters decrease. The decreasing trend of diffusivities through the same membrane increases as the cuts become heavier. There is one order of magnitude of variation in effective diffusion coefficient through the 15-nm pore size membranes between the four SFEF fractions and the end-cut. The diffusion coefficients of the same cut vary slightly through three larger membranes, even though the pore size alters more than one order. However, diffusion coefficients through 15-nm pore size membranes are significantly different from those values through the other three membranes. As the average pore size of the typical hydrotreating catalyst is around 15 nm. The hindered diffusion of residue molecules in commercial catalysts will be significant under ambient conditions.

In the previous studies, the whole asphaltenes or residues were used as feedstocks. The relative exact results cannot be obtained because of the large polydispersity of these feedstocks. Our results show that the SFEF fractions are slightly polydisperse in size. Therefore, the average effective diffusion coefficients can be determined and used to quantitatively evaluate the diffusional hindrance for the SFEF fractions through membrane pores.

Bulk diffusion coefficients and average diameters

The bulk diffusion coefficient is the value corresponding to the infinite pore diameter. Exponential approximations have been proposed to correlate the effective diffusion

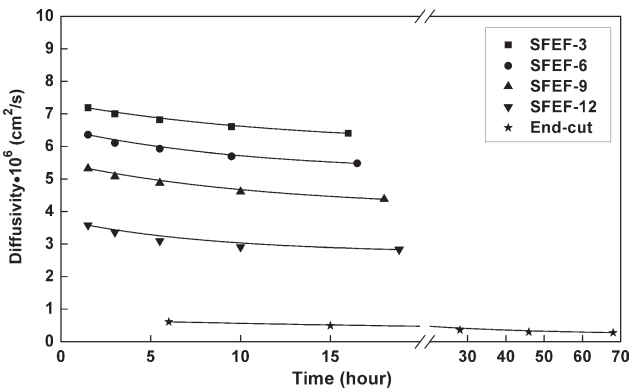

Figure 2. Effective diffusion coefficients of the five cuts in 15-nm pore size membranes.

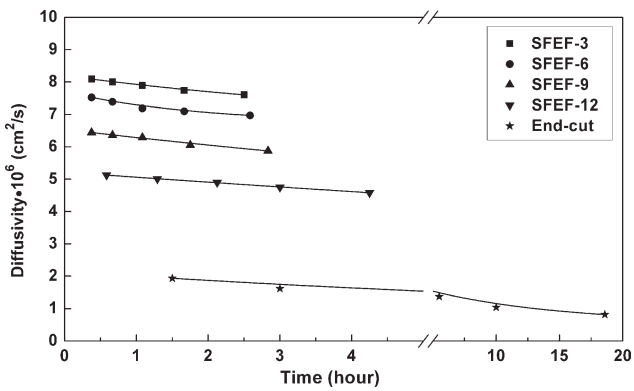

Figure 3. Effective diffusion coefficients of the five cuts in 50-nm pore size membranes.

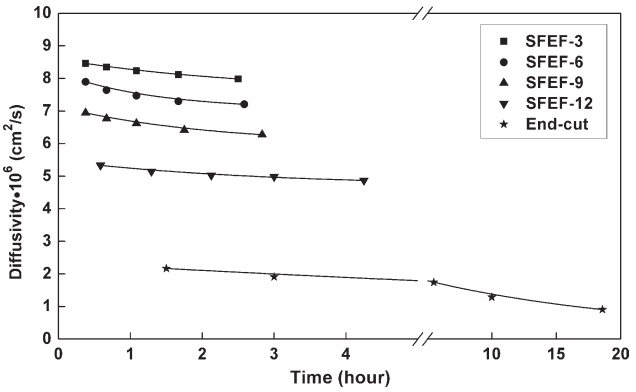

Figure 4. Effective diffusion coefficients of the five cuts in 80-nm pore size membranes.

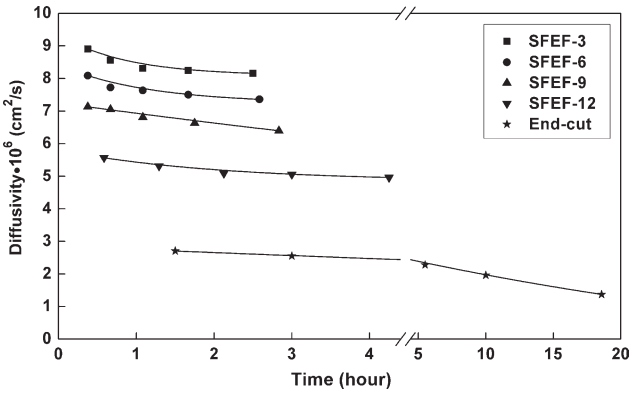

Figure 5. Effective diffusion coefficients of the five cuts in 1000-nm pore size membranes.

coefficient to pore diameter. The bulk diffusion coefficients of the five SFEF cuts can be determined by extrapolating to infinite pore diameter. Figure 6 shows a linear correlation by plotting a semilogarithmic graph of D_e vs. d_p^{-1}. The bulk diffusion coefficients obtained from extrapolation are listed in Table 4. Figure 6 shows that the slopes become steeper as the SFEF cuts become heavier. The diffusion of a heavier cut is hindered more severely by transport through the same membrane. As a result, the larger variation between the bulk and the effective diffusion coefficient for heavier cut are observed.

Table 4 shows that the bulk diffusion coefficients decrease as the cuts become heavier. This trend increases especially for the end-cut. Table 4 also shows that the diffusion coefficients through 1000-nm pore size membranes approach the extrapolated values. Size of residue molecules ranges less than 10 nm.[2,37] Compared with the 1000-nm pores, residue molecules are sufficiently small so that hindered effects are negligible. As a result, the experimental diffusion coefficient for each cut through 1000-nm pore size membranes approaches the bulk value from extrapolation. As mentioned earlier, hydrodynamic diameter can be calculated from the bulk diffusion coefficient by the Stokes-Einstein equation. The hydrodynamic diameters of the five SFEF cuts are also listed in Table 4. The size of the four SFEF fractions increases gradually as they become heavier. However, the size of the end-cut increases sharply. The variations are similar to that of the average molecular weights for these cuts. Good power-law relationships between size and molecular weight for residue have been reported in the literature.[38,39] A regression analysis of our results yields the following relationship:

$$d = 0.028 \times M^{0.57}. \tag{10}$$

Equation 10 fits the experiment data well with an R^2 value more than 0.99. The 0.57 power dependence between d and M is slightly larger than the values reported in the literature.[38–40]

Hindrance factor

A reduction in diffusion coefficient can be observed in Figure 6 as pore diameters decrease and cuts become heavier. Using ln-ln representation, a reasonable linear behavior is shown in Figure 7, from which the following relationship was determined.

$$F(\lambda) = (1 - \lambda)^{4.9}. \tag{11}$$

The hindrance factors of the four SFEF fractions in 15-nm pore size membrane range from 0.54 to 0.79. This indicates that the hindered effect on diffusion for even relatively small residue molecules is very significant. The hindrance factor of the end-cut in 15-nm pore size membranes is estimated to be 0.16. This means that the hindered diffusion of the end-cut is more severe than that of the four SFEF fractions. Although there are small hindered effects for the four narrow SFEF fractions in 50- and 80-nm pore size membranes, the hindered effects for the end-cut in these two membranes are still significant. This implies that the diffusion of AVR molecules is strongly hindered across pores of typical hydrotreating catalysts. Therefore, a number of large pores are required to provide sufficient large channels for easy access into the catalyst by residue molecules.

Table 4. Diffusivities and Average Diameters of AVR Cuts

	$\overline{D_e} \times 10^6$ (cm^2/s)					
Cut	15 nm	50 nm	80 nm	1000 nm	$\overline{D_b} \times 10^6$ (cm^2/s)	$\overline{d}$ (nm)
SFEF-3	6.67	7.76	8.16	8.36	8.42	1.07
SFEF-6	5.82	7.13	7.41	7.56	7.70	1.17
SFEF-9	4.66	6.05	6.48	6.63	6.78	1.33
SFEF-12	2.95	4.62	5.03	5.17	5.43	1.66
End-cut	0.32	1.17	1.40	1.93	1.99	4.54

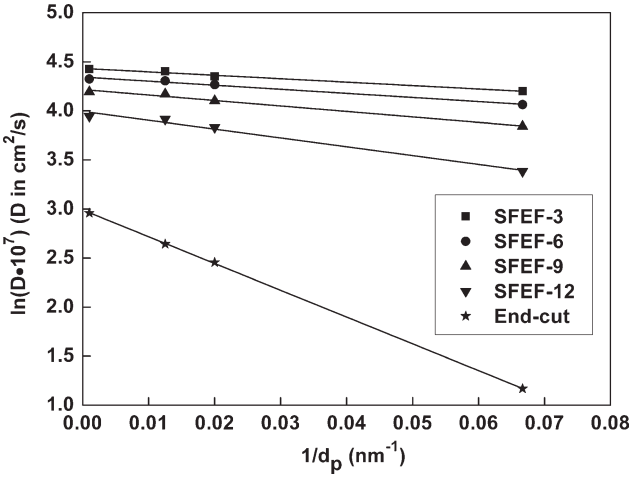

Figure 6. Effective diffusion coefficients vary with pore diameters.

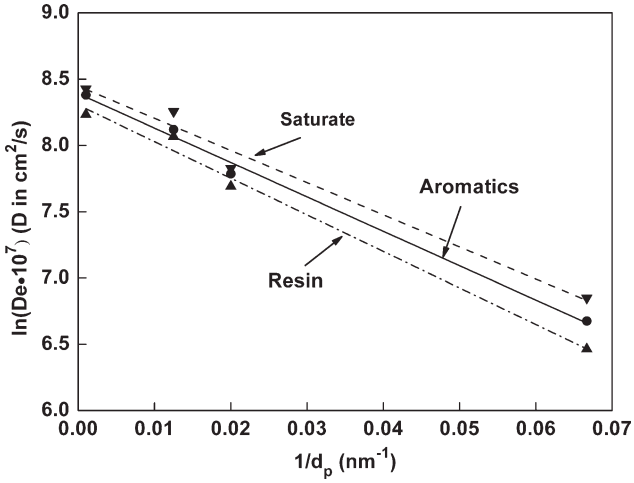

Figure 8. Effective diffusion coefficients of SFEF-3 subfractions vary with pore diameters.

The exponent value 4.9 in Eq. 11 is larger than the value from the Renkin equation, which is about 4.4. This indicates higher hindrance of AVR SFEF cuts than predicted from the Renkin equation. There are two assumptions, solid sphere and centerline drag coefficient, used in the development of the Renkin equation. As seen in reviews by Dechadilok and Deen,[41,42] theories for hindered diffusion have been extended to actual systems, which include nonspherical solutes, noncircular pores, and off-axis solute positions. Centerline approximation appears accurate for diffusion of a sphere in a cylindrical pore. Configuration effects on hindered diffusion have been studied, and the results revealed that diffusivities of nonspherical solutes deviate to predicted values of spherical solutes.[43–45] The difference between our results and those predicted from the Renkin equation might be a result of the configuration effect.

Configuration effect on diffusion

Hindered diffusion of AVR SFEF cuts is more severe than that predicted by the Renkin equation. A recent study indicated that SARA subfractions of the same SFEF fraction have different configurations.[46] SARA subfractions of SFEF-3 were used to evaluate the effect of configuration on diffusion of residue molecules. The average effective diffusion coefficients of three SARA subfractions of SFEF-3 are depicted in Figure 8.

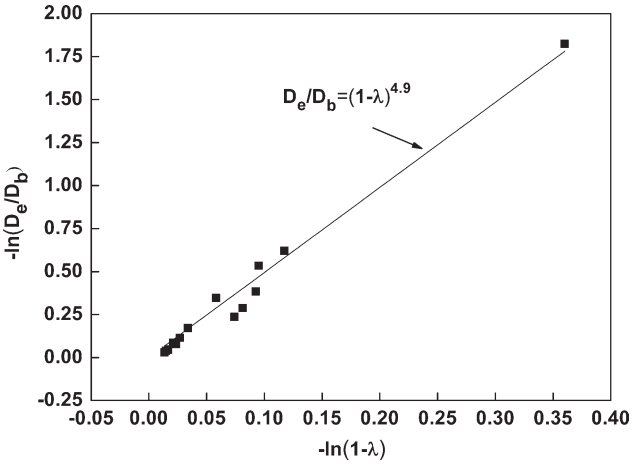

Figure 7. Hindrance factor as a function of the ratio of cuts size and pore size.

The results show that the effective diffusion coefficients differ among the SARA subfractions. Saturate has the largest effective diffusion coefficient, followed by aromatic, and then resin subfractions. The hindrances of diffusion for the three SARA subfractions, which can be seen from the slopes in Figure 8, have the same decreasing trend as the diffusion coefficients. Zhang et al.[46] have found that the average structure of the SARA subfractions in the same SFEF fraction of heavy oil was different. Both aromatic rings and condensation degree increase in reverse of effective diffusion coefficient. The condensation degree of saturate is smaller than that of aromatic and both are smaller than that of resin. Diffusion of crosslinked molecules is hindered more intensively than branched molecules.[47] Bohrer et al.[21] also found that hindrance factors for linear polymers are significantly greater than those for star-branched polymers. As shown in Table 1, AVR is highly aromatic in constitution. The large degree of aromatic condensation might result in diffusion behavior of these cuts nearer to star-branched molecules rather than that of linear molecules.

There are small differences among diffusivities of SARA subfractions for SFEF-3. The subtle differences in diffusivities may result from small variations in the structures among the SARA subfractions, as shown by Zhang et al.[46] It indicates that suitable catalysts need to be chosen to match residues even though their average molecular weight is similar. The effect of configuration on diffusion for residue was not been examined in the previous studies.

Conclusions

Hindered diffusivities of the AVR SFEF cuts across porous membranes were investigated quantitatively by a diaphragm cell. The results showed that effective diffusion coefficients decrease slightly as experimental time increases,

which illustrates that these cuts are polydisperse in size. The average effective diffusivities decrease as cuts become heavier and membrane pores become narrower. The hindrance factor of the end-cut in 15-nm pore size membranes is estimated to be 0.16, corresponding to the variation range of 0.51–0.79 for the four SFEF fractions. This suggests that the diffusion of AVR molecules is strongly hindered across pores of typical hydrotreating catalysts. The results from fitting the experimental data indicate that the hindered degree of the five SFEF cuts is larger than predicted value from the Renkin equation. The different diffusivities of the SARA subfractions for SFEF-3 imply that the effective diffusivities and diffusion hindrance might be influenced by the configuration of residue molecules.

Acknowledgments

The authors acknowledge the support by the National Natural Science Foundation of China through the program for Distinguished Young Scholar (Grant Nos. 20525621 and 20725620) and the National Basic Research Program (Grant Nos. 2004CB217802 and 2004CB217803).

Notation

c = concentration of solution
d = diameter of solute
d_p = diameter of pore
D_e = effective diffusion coefficient of solute
D_b = bulk diffusion coefficient of solute
F = hindered factor of diffusion
l = effective diffusion path length
m = the amount of the solute
M = molecular weight
n = pore density
S = effective diffusion area of the membrane pores
t = time of sampling
T = absolute temperature
V = volume of chamber of diaphragm cell

Greek letters

η = solvent viscosity
κ = Boltzmann's constant
λ = ration of molecule diameter to pore diameter, d/d_p

Subscript

i = the ith SFEF fraction of AVR
j = sampling number
0 = initial state of diffusion experiment
f = finial state of diffusion experiment
L = lower chamber
U = upper chamber

Literature Cited

1. Andrews AB, Guerra RE, Mullins OC, Sen PN. Diffusivity of asphaltene molecules by fluorescence correlation spectroscopy. *J Phys Chem A*. 2006;110:8093–8097.
2. Durand E, Clemancey M, Quoineaud A-A, Verstraete J, Espinat D, Lancelin J-M. 1H Diffusion-Ordered Spectroscopy (DOSY) nuclear magnetic resonance (NMR) as a powerful tool for the analysis of hydrocarbon mixtures and asphaltenes. *Energy Fuels*. 2008;22:2604–2610.
3. Baltus RE, Anderson JL. Hindered diffusion of asphaltenes through microporous membranes. *Chem Eng Sci*. 1983;38:1959–1969.
4. Sane RC, Tsotsis TT, Webster IA, Ravi-Kumar VS. Studies of asphaltene diffusion and structure and their implication for resid upgrading. *Chem Eng Sci*. 1992;47:2683–2688.
5. Sane RC, Webster IA, Tsotsis C. A study of asphaltanes diffusion through unimodal porous membranes. *Stud Surf Sci Catal*. 1988;38:705–716.
6. Sane RC, Tsotsis TT, Webster IA. Hondo asphaltene diffusion in microporous track-etched membranes. Paper presented at the National Meeting of American Chemical Society, Division of Fuel Chemistry, Los Angeles, September 25–30, 1988.
7. Yang X, Guin JA. Diffusion-controlled adsorptive uptake of coal and petroleum asphaltenes in a $NiMo/Al_2O_3$ hydrotreating catalyst. *Chem Eng Commun*. 1998;166:57–79.
8. Yang X, Guin JA. Hindered diffusion of coal and petroleum asphaltenes in a supported hydrotreating catalyst. Paper Presented at the National Meeting of American Chemical Society, Division of Fuel Chemistry, Orlando, August 25–30, 1996.
9. Mieville RL, Trauth DM, Robinson KK. Asphaltene characterization and diffusion measurement. General Papers (Poster Session) Presented Before the National Meeting of American Chemical Society, Division of Petroleum Chemistry, Miami Beach, September 10–15, 1989.
10. Tsai MC, Chen YW, Li C. Restrictive diffusion under hydrotreating reactions of heavy residue oils in a trickle bed reactor. *Ind Eng Chem Res*. 1993;32:1603–1609.
11. Yang C, Du F, Zheng H, Chung KH. Hydroconversion characteristics and kinetics of residue narrow fractions. *Fuel*. 2005;84:675–684.
12. Zhao S, Xu Z, Xu C, Chung KH, Wang R. Systematic characterization of petroleum residua based on SFEF. *Fuel*. 2005;84:635–645.
13. Renkin EM. Capillary and cellular permeability to some compounds related to antipyrine. *Am J Physiol*. 1953;173:125–130.
14. Lee SY, Seader JD, Tsai CH, Massoth FE. Solvent and temperature effects on restrictive diffusion under reaction conditions. *Ind Eng Chem Res*. 1991;30:607–613.
15. Kathawalla IA, Anderson JL. Pore size effects on diffusion of polystyrene in dilute solution. *Ind Eng Chem Res*. 1988;27:866–871.
16. Shao J, Baltus RE. Hindered diffusion of dextran and polyethylene glycol in porous membranes. *AIChE J*. 2000;46:1149–1156.
17. Lee SY, Seader JD, Tsai CH, Massoth FE. Restrictive diffusion under catalytic hydroprocessing conditions. *Ind Eng Chem Res*. 1991;30:29–38.
18. Shi TP, Hu YX, Xu ZM, Su T, Wang RA. Characterizing petroleum vacuum residue by supercritical fluid extraction and fractionation. *Ind Eng Chem Res*. 1997;36:3988–3992.
19. Liang W. *Petroleum Chemistry*, 2nd ed. Dongying: Petroleum University Press, 1995.
20. Macpherson JV, Jones CE, Barker AL, Unwin PR. Electrochemical imaging of diffusion through single nanoscale pores. *Anal Chem*. 2002;74:1841–1848.
21. Bohrer MP, Fetters LJ, Grizzuti N, Pearson DS, Tirrell MV. Restricted diffusion of linear and star-branched polyisoprenes in porous membranes. *Macromolecules*. 1987;20:1827–1833.
22. Baltus RE, Andersen JL. Comparison of g.p.c. elution characteristics and diffusion coefficients of asphaltenes. *Fuel*. 1984;63:530–535.
23. Gordon AR. The diaphragm cell method of measuring diffusion. *Ann N Y Acad Sci*. 1945;46:285–308.
24. Bohrer MP. Diffusional boundary layer resistance for membrane transport. *Ind Eng Chem Fund*. 1983;22:72–78.
25. Holmes JT, Wilke CR, Olander DR. Convective mass transfer in a diaphragm in diffusion cell. *J Phys Chem*. 1963;67:1469–1472.
26. Stokes RH. Integral diffusion coefficients of potassium chloride solutions for calibration of diaphragm cells. *J Am Chem Soc*. 1951;73:3527–3528.
27. Beck RE, Schultz JS. Hindered diffusion in microporous membranes with known pore geometry. *Science*. 1970;170:1302–1305.
28. Stokes RH. An improved diaphragm-cell for diffusion studies, and some tests of the method. *J Am Chem Soc*. 1950;72:763–767.
29. Woolf LA, Tilley JF. Revised values of integral diffusion coefficients of potassium chloride solutions for the calibration of diaphragm cells. *J Phys Chem*. 1967;71:1962–1963.
30. Wu Y, Ma P, Liu Y, Li S. Diffusion coefficients of L-proline, L-threonine and L-arginine in aqueous solutions at 25°C. *Fluid Phase Equilib*. 2001;186:27–38.
31. Smith MJ, Flowers TH, Cowling MJ, Duncan HJ. Method for the measurement of the diffusion coefficient of benzalkonium chloride. *Water Res*. 2002;36:1423–1428.
32. Gosting LJ. A study of the diffusion of potassium chloride in water at 25°C with the Gouy interference method. *J Am Chem Soc*. 1950;72:4418–4422.

33. Sakai M, Yoshihara M, Inagaki M. Hydrodynamic studies of dilute pitch solutions: the shape and size of pitch molecules. *Carbon*. 1983;21:593–596.
34. Andreatta G, Bostrom N, Mullins OC. High-Q ultrasonic determination of the critical nanoaggregate concentration of asphaltenes and the critical micelle concentration of standard surfactants. *Langmuir*. 2005;21:2728–2736.
35. Evdokimov IN, Eliseev NY, Akhmetov BR. Asphaltene dispersions in dilute oil solutions. *Fuel*. 2006;85:1465–1472.
36. Andreatta G, Goncalves CC, Buffin G, Bostrom N, Quintella CM, Arteaga-Larios F, Perez E, Mullins OC. Nanoaggregates and structure-function relations in asphaltenes. *Energy Fuels*. 2005;19:1282–1289.
37. Schneider MH, Andrews AB, Mitra-Kirtley S, Mullins OC. Asphaltene molecular size by fluorescence correlation spectroscopy. *Energy Fuels*. 2007;21:2875–2882.
38. Barre L, Simon S, Palermo T. Solution properties of asphaltenes. *Langmuir*. 2008;24:3709–3717.
39. Nortz RL, Baltus RE, Rahimi P. Determination of the macroscopic structure of heavy oils by measuring hydrodynamic properties. *Ind Eng Chem Res*. 1990;29:1968–1976.
40. Baltus RE. *Characterization of asphaltenes and heavy oils using hydrodynamic property measurements*. In: Mullins OC, Sheu, EY, editor. *Structures and Dynamics of Asphaltenes*. New York: Plenum Press, 1998:X.
41. Deen WM. Hindered transport of large molecules in liquid-filled pores. *AIChE J*. 1987;33:1409–1425.
42. Dechadilok P, Deen WM. Hindrance factors for diffusion and convection in pores. *Ind Eng Chem Res*. 2006;45:6953–6959.
43. Tsai CH, Massoth FE, Lee SY, Seader JD. Effects of solvent and solute configuration on restrictive diffusion in hydrotreating catalysts. *Ind Eng Chem Res*. 1991;30:22–28.
44. Deen WM, Bohrer MP, Epstein NB. Effects of molecular size and configuration on diffusion in microporous membranes. *AIChE J*. 1981;27:952–959.
45. Kathawalla IA, Anderson JL, Lindsey JS. Hindered diffusion of porphyrins and short-chain polystyrene in small pores. *Macromolecules*. 1989;22:1215–1219.
46. Zhang ZG, Guo S, Zhao S, Yan G, Song L, Chen L. Alkyl side chains connected to aromatic units in Dagang vacuum residue and its supercritical fluid extraction and fractions (SFEFs). *Energy Fuels*. 2009;23:374–385.
47. Bohrer MP, Patterson GD, Carroll PJ. Hindered diffusion of dextran and ficoll in microporous membranes. *Macromolecules*. 1984;17:1170–1173.

Manuscript received May 29, 2009, and revision received Oct. 17, 2009.